

Variabilities in the estimate of 100-year return period wave height in the Indian shelf seas

Subal Vinayan^{1,2}, Sanil Kumar V^{1,3*}, Sajeev R²

¹Ocean Engineering, CSIR-National Institute of Oceanography (Council of Scientific & Industrial Research), Dona Paula - 403 004 Goa, India

²Department of Physical Oceanography, School of Marine Sciences, Cochin University of Science and Technology, Lakeside Campus, Fine Arts Avenue, Cochin – 682 016 Kerala, India

³Academy of Scientific and Innovative Research (AcSIR), Ghaziabad -201002, Uttar Pradesh, India

*Correspondence to email: sanil@nio.org

Abstract

Exploring the variability in design wave heights through extreme value analysis is crucial for understanding extreme oceanographic conditions and is paramount for the safe design and operation of offshore structures. This research delves into a comprehensive analysis of wave height variability in the Indian shelf seas, focusing on wave heights for a 100-year return period at 30 locations using 42 years of reanalysis data. The study employs the Generalised Extreme Value distribution and the Generalised Pareto Distribution (GPD), utilizing the annual maxima approach with three methods: maximum likelihood, probability-weighted moments, and moments of probability scale. The GPD Peaks Over Threshold (POT) approach is explored with thresholds estimated using various (91 to 99) percentiles, alongside a graphical approach utilizing threshold determination through mean residual life (MRL) plots. Results indicate that the GPD POT approach, particularly when employing thresholds derived from MRL plots, outperforms other methods. Thresholds obtained by MRL method closely align with the thresholds obtained through the 99-percentile for all locations in the Arabian Sea. This investigation not only enhances our understanding of the dynamic wave processes in the Indian shelf seas but also underscores the efficacy of specific statistical distributions and approaches in the evaluation of design wave heights.

Keywords: generalized extreme value, generalized Pareto distribution, peaks over threshold, return period, wind waves

1. Introduction

The shelf seas of the Indian subcontinent in the Arabian Sea and the Bay of Bengal feature an intricate and dynamic maritime environment with a wide range of oceanographic and climatological events. Understanding design wave heights in this area is essential for the safe operation and sustainable development of coastal and offshore infrastructures. In ocean engineering, the design wave height is a crucial factor for the structural design and safety evaluation of numerous maritime facilities, including ports, harbours, offshore platforms, and coastal protection measures. The initial phase in the design of any marine structure is the extreme value analysis (EVA), which establishes the design wave heights with specific return periods (Goda 2000). With the aid of various distribution models that allow extrapolation within the context of extreme value theory, an estimate of the predicted wave height can be provided using long-term historical wave hindcast data or field observed data (Goda 2000, Coles 2001, Caires 2011). The design of offshore structures and their projected design life are influenced by extreme wave conditions. For offshore construction, knowledge of extreme waves with a return period of 50 or 100 years is crucial. A lower return period would be correlated with lower wave height but higher risk, and vice versa.

Generally, the return values are calculated by fitting the Generalised Extreme Value (GEV) distribution to block maxima (for example, annual maxima) or by fitting the Generalised Pareto distribution (GPD) to exceedances beyond a predetermined threshold value (Davidson and Smith 1990, Coles 2001). Taking into account block maxima and peak over threshold (POT) data points, Coles (2001) went into great length regarding the statistics of extreme value prediction. The duration of the recorded time series has a substantial impact on the accuracy of any methodology for extreme values (Samayam et al. 2017, Jonathan et al. 2021). POT analysis is often preferred over direct analysis of annual maxima since there are multiple occurrences of threshold exceedances per annum (Jonathan et al. 2021). The process of selecting of suitable threshold is the critical step in the POT approach. The bias diminishes while the variance increases if a threshold that is too high is chosen because there is insufficient data above it. By choosing a lower threshold, on the other hand, the variance falls as the number of observations grows and the bias rises. The threshold needs to be high enough for the exceedance to converge to GPD and the POT needs to have enough extreme events left to get a trustworthy GPD estimate (Abild et al. 1992). Madsen et al. (1997) reported that for all practical purposes, GPD provides the most efficient return value estimator in the case of maximum likelihood estimation.

Based on data obtained from MIKE21, a spectral wave model for a site on the central west coast of India, Teena et al. (2012) applied a GEV distribution and GPD to the 31-year wave hindcast

data and retrieved extreme waves for different return periods. Naseef et al. (2019) conducted a similar study in 19 locations covering the Arabian Sea and Bay of Bengal using wave hindcast data for 15 years (1998–2012). Samayan et al. (2017) conducted a comprehensive examination of the reliability of extreme wave models along the Indian coast, employing both GEV and GPD methods to estimate return periods of 30 and 100 years. The outcomes of their study revealed a consistent underestimation of return values in comparison to the maximum values observed in the time series. Specifically, the 30-year return values at all four locations demonstrated a noteworthy trend, exhibiting an average reduction ranging from 10 to 25% when estimated using the GEV and GPD methods. This underestimation implies a potential discrepancy between the modeled predictions and the actual measured maximum significant wave heights (SWH) during the specified return periods. Naseef and Kumar (2017) reported that a single storm in the data can cause a large difference in the extreme value estimates. Naseef and Kumar (2020) observed that the 100-year return level decreases by ~30% when wave height during the two cyclones is removed from the data set. When different block periods ranging from 15 to 39 years are considered, the 50-year return levels range from 5.12 to 8.67 m for GEV with annual maxima data (Kumar and Naseef 2020).

The study by Vanem (2015) focusing on the EVA of waves in a North Atlantic region highlights the inherent unreliability of return value predictions for long return periods, a phenomenon observed even when utilizing the same approach and parametric model. This finding underscores the complexity and challenges associated with accurately estimating extreme wave events, suggesting that factors beyond the chosen methodology play a crucial role in the predictive outcomes. The implications of such unreliability are substantial, particularly in the context of assessing risks and planning for extreme events, emphasizing the need for a nuanced understanding of the limitations and uncertainties inherent in extreme value predictions for waves in the North Atlantic region. Parallel to these observations, Venam (2015) points out that several widely used extreme value techniques are only approximately applicable to finite time series, offering reliability primarily in asymptotic scenarios. Moreover, the reliance on extreme data points in these techniques results in substantially smaller sample sizes compared to methods that incorporate the entire dataset. Consequently, the statistical uncertainty surrounding return value estimations is notably amplified for approaches focusing exclusively on extreme data points. Vinoth and Young (2011) investigation into global estimates of extreme wind speed and wave height, employing the Initial Distribution Method (IDM) and POT approach from a large altimeter dataset, reveals important insights. Notably, the study highlights that when applied to buoy data, IDM and POT analyses produce comparable results. However, theoretical limitations of the IDM are acknowledged, particularly its challenges in accurately modeling the tail of

the Cumulative Distribution Function (CDF) and the potential issues with using non-independent data. The study emphasizes the difficulty in determining the efficacy of IDM due to the absence of an absolute measure for comparative purposes.

The above findings underscore the importance of critically assessing the reliability and accuracy of extreme wave models, especially concerning the potential consequences of underestimating return values. Despite numerous research being done, one has yet to be done that identifies the best method for calculating extreme wave heights for a specific source of assimilation wave hindcast data (Samayan et al. 2017). Earlier studies also indicate that the distributions depend on the selection of a threshold value for a location and hence, the main problem is how to select the threshold for a location without loss of data.

The primary objective of the present study is to estimate the design wave heights for a return period of 100 years at 30 specific locations within the Indian shelf seas, each situated around 50 m water depth, employing two distinct statistical distributions: the GEV Distribution and the GPD. Furthermore, the present study endeavours to comprehensively evaluate and compare the performance of these two distribution models to discern which one provides a more accurate and reliable representation of the intricate and region-specific wave height characteristics inherent to the Indian shelf seas, thus aiding in the enhancement of oceanographic modelling and the safety of coastal and offshore infrastructure development in this dynamic maritime environment. This paper is structured as follows. In section 2 details of data and methods used are introduced including the choice of threshold adopted in the study. Section 3 gives a brief explanation of the results obtained by GEV and GPD analysis with different methods and section 4 presents the conclusion.

2. Data and methodology

2.1. Data

The significant wave height (SWH) at 30 locations around 50 m water depth (Figure 1) was obtained for every 1-h interval for the Indian Shelf seas from 1979 to 2020 from the ERA5 reanalysis data produced by the European Centre for Medium-Range Weather Forecasts (ECMWF) and used in the study. With a spatial resolution of 31 km for atmospheric variables, the ERA5 is the fifth generation of ECMWF reanalysis of the global climate (Hersbach et al. 2020). Fanti et al. (2023) compared ERA5 reanalysis data with 326 coastal buoys and ERA5 reanalysis demonstrate a very strong correlation for SWH against the 326 coastal buoys, with mean Pearson correlation coefficients of 0.90 (all reported R values are statistically significant for $p\text{-value} < 0.01$). Anusree and Kumar (2023) compared ERA5 reanalysis data with buoy data in coastal waters in India and the analysis indicates a strong positive

correlation (r-value greater than 0.80) between the measured SWH and the ERA5 data. Previous studies have used ERA5 reanalysis data for conducting extreme value analysis of waves (Naseef and Kumar 2017, Alsaq and Shamji 2022, Siadatmousavi 2023 and Wenyan et al. 2024). Among the selected 30 locations, 16 locations are in the Arabian Sea and 14 locations are in the Bay of Bengal. The present study focuses on the SWH for 42 years with 3,68,184 data points. ETOPO1 (earth topography-1 minute) is used to create the bathymetry presented in Figure 1 (Amante and Eakins 2009).

2.2. Methodology

Two extreme value distributions, the GEV distribution and the GPD, are used to estimate the wave height for a 100-year return period. Statistical distributions fitting and estimation of parameters were performed using routines in WAFO (2000) developed by faculty of engineering, Mathematical Statistics, Lund University, Sweden. WAFO is a toolbox designed for analysing random waves and loads, with sub-toolbox dedicated to extreme value analysis. By defaults WAFO toolbox uses 95% confidence interval for its estimates. Several studies have employed the WAFO toolbox for extreme value analysis of waves (Teena et al. 2012, Alsaq and Shamji 2022, Bulteau et al. 2013).

2.2.1 GEV

Jenkinson (1955) combined the Gumbel, Frechet, and Weibull families into a single family of models called the Generalised Extreme Value family of Distribution.

$$F(X; k, \alpha, \beta) = \begin{cases} e^{-[1-k(\frac{x-\beta}{\alpha})]^{\frac{1}{k}}} & k \neq 0 \\ e^{-e^{-\frac{x-\beta}{\alpha}}} & k = 0 \end{cases} \quad (1)$$

where k is the shape parameter, α is the scale parameter and β is the location parameter. The Gumbel distribution corresponds respectively to the cases $k = 0$, the Frechet distribution corresponds respectively to the cases $k > 0$, and the Weibull distribution corresponds respectively to the cases $k < 0$.

In this study, GEV distribution with Annual Maxima (AM) is used to estimate the return level using three methods; i) Probability Weighted Moments (PWM), ii) Maximum Likelihood (ML) estimation and iii) Maximum Product of Spacing (MPS). The generic Block Maxima approach is where the AM method originates. It entails dividing the data period into regular segments and taking the highest value into account for each. The method is known as the AM method in the specific scenario where this duration equals one year. The return level X_T for once in every return period of T years which is given for GEV as (Palutikof et al. 1999):

$$X_T = \begin{cases} \beta + \frac{\alpha}{k} \left\{ 1 - \left[-\ln \left(1 - \frac{1}{T} \right) \right]^k \right\} & k \neq 0 \\ \beta - \alpha \ln \left[-\ln \left(1 - \frac{1}{T} \right) \right] & k = 0 \end{cases} \quad (2)$$

2.2.2 GPD

The drawback of GEV distribution is that it considers only one peak in each block which ignores other extreme events that occurred in that block. To overcome this drawback GPD method incorporated with the POT approach is used, which extracts values exceeding a sufficiently high threshold and eliminates values below that. The GPD function is,

$$F(X; k, \alpha, \beta) = \begin{cases} 1 - \left(1 - k \frac{x-\beta}{\alpha} \right)^{1/k} & k \neq 0 \\ e^{-e^{-\frac{x-\beta}{\alpha}}} & k = 0 \end{cases} \quad (3)$$

The return level X_T for once in every return period of T years is estimated using the equation:

$$X_T = \begin{cases} k + \frac{\alpha}{k} [1 - (\lambda T)^{-k}] & k \neq 0 \\ k + \alpha \ln(\lambda T) & k = 0 \end{cases} \quad (4)$$

where λ is threshold crossing rate, expressed as N_u/N . The N_u is the overall number of exceedances over the chosen threshold U , N is the overall number of record years, and k is the fitted GPD parameters to the data exceedances $x-u$.

2.2.3 Threshold Selection

The selection of a threshold is a critical step in EVA, particularly when fitting a GPD to model extreme events. The choice of threshold can significantly impact the results of your analysis, including the estimated parameters of the GPD and the reliability of predictions. The choice of thresholds is crucial to the Peaks Over Threshold (POT) approach framework from a theoretical perspective, which is why in the past decade numerous methodologies have been proposed for its selection (Benito et al. 2023). In this study, threshold selection for GPD analysis is done by two methods: the first method is a statistical method known as percentile method (threshold selection using percentile) and the second one is a graphical method known as Mean Residual Life (MRL) plot method.

In the percentile method, multiple percentiles were considered to comprehensively capture at different levels of extremity within the data evidence suggests that data points exceeding higher thresholds exhibit a stronger compatibility with the GPD compared to those exceeding lower thresholds. As a result, it is advisable to select a threshold that is as high as practical while ensuring

the availability of a sufficient number of data points for meaningful analysis (Viselli et al. 2015). Recognizing the critical role of threshold selection in capturing extreme events accurately, a range of percentiles was considered, specifically at the 91, 93, 95, 97 and 99 percentiles. These percentiles were chosen to assess varying levels of extremeness and to provide a comprehensive view of the tail behaviour of data. The sample numbers corresponding 91, 93, 95, 97 and 99 percentiles are 33087, 25734, 18373, 11022 and 3675 respectively. The selection of multiple percentiles allows for exploring the sensitivity of the analysis to different threshold choices and evaluating their impact on the estimation of return values. Each chosen percentile served as a threshold above which extreme wave heights are analysed by GPD with the MPS method.

The second method MRL plot is a graphical method in which the threshold is identified from a plot of mean excess against a range of thresholds.

$$\{(u, e_n(u)), X_{n:n} < u < X_{1:n}\} \quad (5)$$

Where $X_{1:n}$ and $X_{n:n}$ represent the initial and final order statistics respectively, of the given data sample, u is the threshold and $e_n(u)$ is the sample mean excess function i.e., the summation of excess over threshold u , divided by the count of data points that surpass the specified threshold u , defined by

$$e_n(u) = \frac{\sum_{i=1}^n (X_i - u)}{\sum_{i=1}^n 1(X_i > u)} \quad (6)$$

The empirical estimate of the mean excess function, denoted by $e_n(u)$, corresponds to the mean excess function itself, represented as $e(u) = E[X - u \mid X > u]$. Specifically, When the empirical plot exhibits a reasonably linear trend with a positive slope beyond a certain threshold value u , it suggests that the excess over this threshold adheres to a GPD with a positive shape parameter (McNeil and Saladin 1997). The threshold is estimated from the MRL plot by both mean residual analysis and manual visual inspection. Although the POT method is primarily aimed at facilitating the selection of an independent identically distributed dataset, it is advisable to ensure that this prerequisite is met. So that a dataset for POT was extracted by implementing a separation time to safeguard the independence of extremes. An interval of 96 hours between each peak is chosen to regard them as independent events.

The fit of different distributions to the data was checked by using a residual quantile plot and root mean square error (RMSE). The residual quantile plot is a graphical tool for determining whether a sample originates from a particular distribution. In particular, a comparison between the quantiles of an empirical distribution and a hypothesised distribution is made. The plot will be linear if the data originates from the specified distribution, other distribution types will introduce curvature in the plot. A very low RMSE (close to 0) indicates an excellent fit of the model to the data.

3. Results

Among the locations studied, the largest annual maximum SWH of 7.97 m was observed during May 1990 at location L23 (81.50°E, 16.00°N) in Bay of Bengal off the east coast of India and a minimum annual maximum SWH of 3.00 m was observed at location L13 in the Arabian Sea off the southwest coast of India (Table 1). The annual average SWH varied from 0.80 m (at L13) to 1.49 m (at L16) in the locations of the west coast of India and from 0.66 m (at L21) to 1.19 m (at L30) in the locations of the east coast of India.

3.1 GEV Method

At the selected significance level of 5%, there is insufficient evidence to reject the null hypothesis that the annual maximum values adhere to the Gumbel distribution (Bhaskaran et al. 2023). Return value estimation at 30 locations using GEV distribution by using AM extracted from the hourly SWH data using three methods: MPS, ML and PWM are presented in Table 1. Figure 2 shows the AM for 30 locations in the Indian shelf seas which were extracted from the SWH dataset to be used in the block-maxima approach. The highest average annual maximum SWH of 4.41 m was observed in L30 and the lowest average annual maximum of 2.16 m was observed in L13. The return level estimates for each location unveil the influence of the chosen method on the outcomes. The highest percentage variation of return level relative to observed SWH using the ML method is 57.84% at L20, while the PWM method records the maximum percentage variation of 26.71% in return level relative to the observed SWH at L30 and the MPS method exhibits a percentage increase of 66.12% in return level from SWH, notably identified at L30. The residual quantile plot of 30 locations shows a good fit with all three methods (Figures not shown). Typical plots for locations L6 and L20 are shown in Figure 3. The residual quantile plot for L6 displayed the best fit, affirming the adequacy of the chosen distribution for representing the observed data. However, at L20, deviations from the fit line were noted, signalling a potential issue with the fit in this specific location (Figure 3). L6 was chosen because it represents a location where the residual quantile plot displayed an excellent fit, indicating that the chosen distribution adequately represents the observed data. L20 was selected as it demonstrated some deviations from the fit line, highlighting areas where the model's performance might be less reliable. In L20, the return levels estimated by the ML and MPS methods exhibit a slight elevation compared to the observed SWH, with ML showing a 57.84% increase and MPS indicating a 63.06% increase. In contrast, the PWM method provides a more conservative estimate in L20, with the return level being 25.56% higher than the observed SWH. For L6, ML demonstrates a modest 4.67% increase, MPS shows a 9.86% increase, and PWM maintains a conservative estimate with a 4.32% increase from the observed SWH. These variations highlight the method-specific discrepancies

in return level estimations, emphasizing the importance of method selection in accurately capturing extreme values across different locations. RMSE values estimated with all methods are in an acceptable range. Thus, the estimation of design wave height for a 100-year return period using GEV distribution holds good. But in some locations, the observed SWH exceeds the estimated design wave height even estimated with three different methods which is not a good result. The estimated design wave height using PWM is 85% to 126% of the maximum observed SWH at different locations, whereas for ML, it is 82% to 157% and for MPS, it is 88 to 166% (Figure 4a). Estimated RMSE values show that the PWM method shows much better results than the ML and MPS methods. The RMSE values for L15 are 0.0409 using MPS, 0.027 using PWM, and 0.0271 using ML methods, while for L20, the values are 0.5168 using MPS, 0.477 using ML, and 0.2579 using PWM methods. It is evident that the PWM method demonstrates superior performance in GEV modeling compared to the MPS and ML methods for both L15 and L20, as evidenced by its notably lower RMSE values. Figure 5a, shows the return levels at 30 locations, computed using the GEV PWM method with annual maxima SWH data from distinct time periods 30 years (1979-20008), 42 years (1979-2020), and the recent 30 years (1991-2020). From L1 to L19, the return levels estimated by all three datasets are notably similar, indicating a consistency in extreme wave events across these locations over different time periods. A significant discrepancy is observed at location L23. The return levels estimated using 1979-2002 and 1979-2020 dataset show a substantial peak compared to the return level estimated from the 1991-2020 dataset. This discrepancy can be attributed to the exclusion of the 1990 cyclone and similar events occurred in the Andhra Pradesh coast in the 1991-2020 dataset. In locations from L19 – L30, return level estimated using 1979-2008 dataset underestimates return level when compared to the 1979-2020 and 1991-2020 datasets, except at L22, L23 and L24, where the return levels either show a significant peak or lie closer to those estimated by the other two datasets. Figure 5b presents the return levels estimated using the GEV PWM method, along with the corresponding 95% confidence intervals.

3.2 GPD POT Approach

In the first method a range of thresholds has been selected using the percentile method and the design wave height has been estimated using that threshold (Table 2). According to Salcedo-Castro et al. (2018), the 93, 95, and 97 percentiles could be employed for the estimation of the return period. In the present study, the thresholds were chosen from a quantile range between the 91 and the 99 percentiles at 2% increments. A threshold that is significantly less than the 91 percentiles cannot be selected because that may result in including a large number of less extreme events. The choice of percentiles for threshold selection depends on the specific application and the balance between the risk of underestimating extreme events and the risk of overestimating them. The selection of the percentile

may also depend on the available data, the specific goals of the analysis, and the acceptable level of risk in the decision-making process. In some cases, a sensitivity analysis can be performed using different percentiles to understand the impact of threshold selection on the results.

The result shows that in some locations, the observed SWH exceeds the estimated design wave height and in some locations, the estimated design waves exceed too much than the observed SWH which tested with all ranges of threshold estimated with different percentiles (Figure 4b). In the context of wave analysis, from L1 to L17 in the Arabian Sea, when using thresholds estimated with the 91, 93, 95, 97 and 99 percentiles, the result reveals that the estimated return level is either less than or approximately equal to the observed maximum SWH in that region. Such an outcome is deemed unacceptable, as it indicates an inconsistency between the estimated values and the real observations. However, from L18 to L30 in the Bay of Bengal, using the same percentiles for threshold estimation, the picture changes dramatically. Here, the estimated return levels exhibit a sudden increment, and some of them are found to be within an acceptable range. However, there are instances where the estimated values exceed the observed SWH by a considerable margin, making them untenable for practical purposes. In the case of locations L20, L22 and L28, utilising thresholds estimated across all five percentiles (91, 93, 95, 97 and 99) led to return level estimations that significantly deviated from the observed SWH. The highest percentage variation in return level relative to observed SWH is observed at L22, employing thresholds at 91, 93 and 95 percentiles, corresponding to 212%, 236% and 268%, while employing the 97 percentile threshold highest percentage variation of return level is 258% which is observed at L20 and a variation of 398% is observed at L23 when 99 percentiles is considered. For location L23, the return level obtained with the 91 percentile threshold is close to the observed maximum SWH value. This emphasises the sensitivity of the threshold parameter, where even slight variations can exert a substantial impact on the results. The percentile method, in particular, demonstrated a reduced level of accuracy when applied in the context of the Indian Ocean. Also, the residual quantile plot (empirical vs the modelled data) of two typical locations L15 and L22 are presented in Figure 6. The residual quantile plot of L15 shows a better fit, while the fit is not good in L22 while employing thresholds at 91, 93, 95 and 97 percentiles in both locations (Figure 6). In locations L20, L22 and L28, data is not showing good fit, which shows poor fit in residual quantile plot while employing modelled data and empirical data for these locations.

In the second method threshold is graphically estimated using an MRL plot, in which the threshold is selected by mean residual analysis (Figure 7a). The mean residual life method employed to determine the optimal threshold has produced results that closely align with or fall within the estimated bounds obtained through the block-maxima approach (Bhaskaran et al. 2023). Choosing an

appropriate threshold value is essential for accurate estimates of the extreme value analysis with respect to GPD. The threshold values chosen for each location, using the mean excess approach, were sufficiently high to allow for independent observations and to converge the POT analysis into GPD (Alsaq and Shamji 2022). Several factors are involved in this strategy, including the minimum number of extremes, the minimum distance between extremes, and the block period. Since fewer points would result in a poor fit to the GPD, the minimum number of extremes was fixed at 20 (Simiu and Heckert 1996). Declustering extreme data necessitates a minimum distance between extremes, which often falls between two and fourteen days (Simiu and Heckert 1996). Because it provides a tighter confidence interval, the minimum distance between extremes was set at 96 hours i.e., 4 days (Viselli et al. 2015). One year was chosen as the block period. The estimation of the return level was done with the chosen threshold from the mean residual analysis. While the return level estimation with selected thresholds yielded satisfactory results for the majority of the 30 locations, certain areas displayed discrepancies. Specifically, some locations reported return levels lower than the observed maximum SWH, while an outlier, location L23, exhibited an unacceptably significant deviation, surpassing the observed SWH by a considerable margin. The fit was not good for most of the locations when tested with residual quantile plot and also for some locations unacceptable RMSE values were obtained. The same return levels were observed while estimating the threshold by decreasing the distance between extremes to 72 and 48 hours. Earlier studies also indicate that the POT approach results were dependent on the selected time window at lower thresholds, while the results for bigger thresholds were unaffected by the time window (Bhaskaran et al. 2023). The threshold selected from the MRL plot manually for a location is shown in Figure 7b. The threshold is identified when the plot appears to follow a positive linearity over a specific value which indicates that the excesses above this threshold follow a GPD with a positive shape parameter (McNeil and Saladin 1997). The sensitivity of threshold selection in the analysis was readily apparent, emphasising the critical role of this parameter. Initially, an arbitrary approach was adopted, with the threshold chosen based on a random positive peak from the MRL plot. However, this unconventional method yielded unexpected and unfavourable outcomes. It produced notably poor return values, resulting in a high RMSE and an ill-fitting residual quantile plot. From the residual quantile plot itself, a large bias is observed with empirical data (Figure 7c).

Recognizing the need for a more systematic and data-driven threshold determination process, a comprehensive and meticulous approach was undertaken. Instead of relying on a single threshold, the dataset was explored more thoroughly. Multiple positive peaks were considered as potential candidates, and each was tested as a threshold (Figure 7b). This extensive and methodical exploration led to the selection of a threshold that ultimately provided the most promising results. The revised

approach yielded significant improvements in return level estimation. Furthermore, the results demonstrated a much better fit in the residual quantile plot, signifying a closer alignment with the underlying data distribution (Figure 7d). The maximum percentage variation in return level while relating with observed SWH is 38.99% which is observed at L22. Additionally, the RMSE value significantly decreased, reflecting a higher degree of accuracy in the model's predictions. In summary, the in-depth examination of multiple threshold candidates culminated in the identification of the most suitable threshold, significantly enhancing the robustness and precision of the analysis.

The return level has been estimated using the selected threshold and presented in Table 2. Maximum and minimum return levels and corresponding location have been identified, maximum return level estimated is 9.68 m at location L23 and minimum return level estimated is 3.32 m, which is at location L13. This approach led to well-fitting residual quantile plots (Figure 7d) and produced design wave heights that consistently aligned with the observed data. The estimated design wave height using MRL is 104 % to 138% of the maximum observed SWH at different locations, whereas the values based on different percentiles, it is 78% to 367% (Figure 4b). Notably, the discrepancies between the estimated and observed wave heights were minimal, with no instances of excessive overestimation for MRL. This level of precision was further substantiated by remarkably low RMSE values, underscoring the effectiveness and reliability of the GPD method when employing the MRL-derived threshold for design wave height estimation. In the GPD MPS method, return levels estimated using thresholds derived from the MRL method exhibit consistently lower RMSE values compared to those derived from the percentile method for L15 (0.007 for MRL vs. 0.0069-0.0083 for percentile), L20 (0.0459 for MRL vs. 0.0672-0.3175 for percentile), and L22 (0.0377 for MRL vs. 0.0973-0.1658 for percentile). This highlights the superior performance of GPD with MRL-derived thresholds in accurately estimating return levels across various return periods. In fact, the RMSE values were consistently smaller than those achieved by all three methods within the GEV framework and the percentile method, highlighting the superior performance of the GPD approach in the estimation of design wave height in the Indian shelf seas. The percentage variation in the return levels obtained following GEV with different methods compared to that from the GPD MRL plot is presented in Figure 4c and between GPD with thresholds 91, 93, 95, 97 and 99 percentiles with MRL plot is presented in Figure 4d. Thresholds estimated by MRL method closely align with the thresholds obtained through the 99-percentile method for all locations in Arabian Sea and location L17 as depicted in Figure 4. However, beyond L17 and extending to L30, significant deviations are observed in comparison to the MRL method, distinguishing it from the outcomes generated by all other methods.

4 Discussion

The study demonstrates that the GPD method, especially when using the MRL-derived threshold, outperforms the GEV approach in accurately estimating design wave heights in all locations. The GPD method with MRL derived threshold provides design wave height estimates that closely match the observed data without significant overestimation, offering a more robust solution for coastal engineering and wave height forecasting. When comparing return levels estimated using GEV-ML, PWM and MPS methods with GPD-MRL method, the PWM method shows less variation than other two methods, while comparing GPD percentiles with GPD-MRL return level estimated with 91 percentile shows minimum variation. The RMSE obtained from different methods are compared in Figures 5c and 5d. The results show that, in GEV analysis the PWM method shows less RMSE than the ML and MPS methods. With far lower RMSE, the GPD MRL Plot approach performs better than PWM (Figure 5c). When comparing RMSE of GPD MRL Plot approach with GPD POT percentile methods at 91st, 93rd, 95th, 97th, 99th percentiles, shows approximately equal RMSE up to L16. From L17 onwards RMSE values of GPD MRL plot method are significantly lower, indicating the better performance, except at L23 (Figure 5d). The study also indicates that the EVA in the Indian Ocean benefits from a multifaceted approach. Given the complexity and variability of wave conditions observed in the 30 studied locations, relying on a singular method may not suffice for accurate estimations. Consequently, employing diverse methods allowed for a more nuanced understanding of extreme wave characteristics across the examined sites. Shamji et al. (2020) reported that the GPD with POT method is more significant and reliable for estimating design wave height around the Farasan Islands in the southern Red Sea, revealing significant trends in near extremes (90 and 95 percentile SWH) in offshore regions around the Farasan Islands, contrasting with non-significant trends in the nearshore regions. Bekali et al. (2021) reported that the analysis at three points along the Atlantic coast of northern Morocco revealed a difference of less than 10% between results obtained by annual maxima and POT methods, emphasizing necessity of applying both statistical methods for ensuring the safe dimensioning of maritime structures. Agarwal et al. (2013) prepared 100-year return level map of north Atlantic Ocean which reported utilizing GPD to fit all excesses above a high threshold produced more robust estimates of return values than the approach of fitting GEV to storm maxima.

5 Conclusion

In the culmination of this investigation focused on estimating design wave heights for a 100-year return period at 30 specified locations in the Indian shelf seas, profound insights have been gained into the dynamic wave characteristics of this region. The study provides a meticulous evaluation of the effectiveness of two reliable statistical distributions—the Generalised Extreme Value Distribution

(GEV) and the Generalised Pareto Distribution (GPD) in modeling the complex wave height characteristics unique to the Indian shelf seas.

Significantly, findings indicate that the GPD method consistently outperforms the GEV approach, particularly when employing the manually selected threshold derived from the MRL plot. Design wave height with GPD using MRL is 82 to 126% of the value from GEV using PWM. The estimated design wave height using MRL is 103% to 138% of the maximum observed SWH at different locations. Thresholds estimated by the MRL method closely align with the thresholds obtained through the 99-percentile value for all locations in the Arabian Sea. The GPD's remarkable capacity to precisely predict design wave heights across all tested locations is highlighted, presenting a solution that closely aligns with observed data and minimizes the risk of overestimation. In the context of the dynamic maritime environment of the Indian shelf seas, this result holds substantial implications for enhancing the resilience and reliability of coastal engineering and wave height predictions.

Moreover, the analysis of RMSE values and residual quantile plots further underscores the performance disparities between the methods. GEV annual maxima approach exhibits a good fit in residual quantile plots and favourable RMSE values, affirming its competence in capturing the variability of wave height data. Notably, the GPD POT approach, especially when coupled with the MRL-derived threshold, not only provides a good fit in residual quantile plots but also significantly improves RMSE values. This comprehensive assessment reaffirms the efficacy of the GPD method, particularly when guided by MRL-derived thresholds, as a robust and precise tool for predicting design wave heights in the Indian shelf seas. The return levels estimated using datasets covering the entire period from 1979 to 2020 and that from 1991 to 2020 shows large difference in areas influenced by tropical cyclones.

Acknowledgements

The authors gratefully acknowledge the Director, CSIR-National Institute of Oceanography, Goa for the facilities to conduct this research. ERA5 data used in this study have been obtained from the European Centre for Medium-Range Weather Forecasts data server: <http://data.ecmwf.int/data>. We thank both the reviewers for their valuable comments which improved the scientific content of this paper. This is NIO contribution ---.

Author Contributions:

Subal Vinayan: Conceptualization; Data curation; Formal analysis; Methodology; Visualization; Writing - original draft

Sanil Kumar: Conceptualization; Resources; Supervision; Writing - review & editing.

Sajeev R: Writing - review & editing

Funding: External funding was not received for the research.

Conflicts of Interest: The authors declare no conflicts of interest.

References

- Abild J, Andersen EY and Rosbjerg D (1992) The climate of extreme winds at the Great Belt, Denmark. *Journal of Wind Engineering and Industrial Aerodynamics* 41, 521–532. [https://doi.org/10.1016/0167-6105\(92\)90458-M](https://doi.org/10.1016/0167-6105(92)90458-M).
- Agarwal A, Venugopal V and Harrison GP (2013) The assessment of extreme wave analysis methods applied to potential marine energy sites using numerical model data. *Renewable and Sustainable Energy Rev.* 27, 244–257. <https://doi.org/10.1016/j.rser.2013.06.049>.
- Alsaq F and VR S (2022) Extreme Wind Wave Climate off Jeddah Coast, the Red Sea. *Journal of Marine Science and Engineering* 10(6), 748. <https://doi.org/10.3390/jmse10060748>
- Amante C and Eakins BW (2009) ETOPO1 arc-minute global relief model: procedures, data sources and analysis. NOAA technical memorandum NESDIS NGDC, 24 <https://repository.library.noaa.gov/view/noaa/1163>
- Anusree A and Kumar VS. (2024) Mean wave direction and wave height in the ERA5 reanalysis dataset: Comparison with measured data in the coastal waters of India. *Dynamics of Atmospheres and Oceans*, 107, 101478. <https://doi.org/10.1016/j.dynatmoce.2024.101478>
- Bakali H, Serhir N and Aouiche I (2021) Comparison Between Maximum Annual and Peak Over Threshold Methods for the Determination of Extreme Waves in Moroccan Atlantic Coast. In *IOP Conference Series: Earth and Environmental Science* (Vol. 849, No. 1, p. 012002). IOP Publishing. 10.1088/1755-1315/849/1/012002
- Benito S, López-Martín C and Navarro M.Á (2023) Assessing the importance of the choice threshold in quantifying market risk under the POT approach (EVT). *Risk Management*, 25(1), 6. <https://doi.org/10.1057/s41283-022-00106-w>
- Bhaskaran S, Verma AS, Goupee AJ, Bhattacharya S, Nejad AR and Shi W (2023) Comparison of Extreme Wind and Waves Using Different Statistical Methods in 40 Offshore Wind Energy Lease Areas Worldwide. *Energies* 16(19), 6935. <https://doi.org/10.3390/en16196935>
- Bulteau T, Lecacheux S, Lerma AN, Paris F (2013) September. Spatial extreme value analysis of significant wave heights along the French coast. In *International short conference on advances in extreme value analysis and application to natural hazards: EVAN2013*. Siegen, Germany. hal-00857627, <https://brgm.hal.science/hal-00857627>
- Caires S (2011) Extreme value analysis: wave data. Geneva, Switzerland, World Meteorological Organization/JCOMM, 33pp. (JCOMM Technical Report 57). DOI: <https://doi.org/10.25607/OBP-1499>
- Coles S, Bawa J, Trenner L and Dorazio, P (2001) *An Introduction to Statistical Modeling of Extreme Values*. London, UK.: Springer-Verlag, p.

- Davison AC and Smith RL (1990) Models for exceedances over high thresholds. *Journal of the royal statistical society series b-methodological* 52, 393-425. <https://doi.org/10.1111/j.2517-6161.1990.tb01796.x>
- Du Wenyan, Zhang X, Shi H, Li G, Zhou Z, You Z and Zhang K (2024) Long-Term Extreme Wave Characteristics in the Water Adjacent to China Based on ERA5 Reanalysis Data. *Journal of Ocean University of China*, 23(1), pp.1-10. <https://doi.org/10.1007/s11802-024-5446-y>.
- Goda Y (2000) *Random Seas and Design of Maritime Structures*. Advanced Series on Ocean Engineering. 33. 10.1142/3587.
- Fanti V, Ferreira Ó, Kümmerer V and Loureiro, C (2023). Improved estimates of extreme wave conditions in coastal areas from calibrated global reanalyses. *Communications Earth & Environment*, 4(1), 151. <https://doi.org/10.1038/s43247-023-00819-0>.
- Hersbach H, Bell B, Berrisford P, Hirahara S, Horányi A, Muñoz-Sabater J, Nicolas J, Peubey C, Radu R, Schepers D, Simmons A, Soci C, Abdalla S, Abellan X, Balsamo G, Bechtold P, Biavati G, Bidlot J, Bonavita M and Chiara G (2020) The ERA5 global reanalysis. *Quarterly Journal of the Royal Meteorological Society* 146, 1999–2049. <https://doi.org/10.1002/qj.3803>
- Jenkinson AF (1955) The frequency distribution of the annual maximum (or minimum) values of meteorological elements. *Quarterly Journal of the Royal Meteorological Society* 81(348), 158-171. <https://doi.org/10.1002/qj.49708134804>
- Jonathan P, Randell D, Wadsworth J and Tawn, J (2021) Uncertainties in return values from extreme value analysis of peaks over threshold using the generalised Pareto distribution, *Ocean Engineering* 220, 107725, <https://doi.org/10.1016/j.oceaneng.2020.107725>.
- Madsen H, Rasmussen PF and Rosbjerg D (1997) Comparison of annual maximum series and partial duration series methods for modeling extreme hydrologic events: 1. At site modeling. *Water Resources Research* 33, 747–757.
- McNeil AJ and Saladin T (1997) The peaks over thresholds method for estimating high quantiles of loss distributions. In *Proceedings of 28th international ASTIN Colloquium* (Vol. 23, p. 43). <https://api.semanticscholar.org/CorpusID:15645385>.
- Naderi A and Siadatmousavi SM (2023) Extreme value analysis for waves in the Persian Gulf: Skill assessment of different methods for a fetch-limited basin. *Regional Studies in Marine Science*, 59, 102812. <https://doi.org/10.1016/j.rsma.2023.102812>.
- Naseef TM and Kumar VS (2017) Variations in return value estimate of ocean surface waves – a study based on measured buoy data and ERA-Interim reanalysis data. *Nat Hazard Earth Sys* 17, 1763–1778. <https://doi.org/10.5194/nhess-17-1763-2017>.
- Naseef TM and Kumar VS (2020) Influence of tropical cyclones on the 100-year return period wave height—A study based on 39-year long ERA5 reanalysis data. *Int J Climatol*. 40, 2106–2116. <https://doi.org/10.1002/joc.6321>
- Naseef TM, Kumar VS, Joseph J and Jena BK (2019) Uncertainties of the 50-year wave height estimation using generalized extreme value and generalized Pareto distributions in the Indian Shelf seas, *Natural Hazards* 97(3), 1231-1251, doi.org/10.1007/s11069-019-03701-5

- Palutikof JP, Brabson BB, Lister DH and Adcock ST (1999) A review of methods to calculate extreme wind speeds. *Meteorological Applications* 6(2), 119–132.
- Salcedo-Castro J, da Silva NP, de Camargo R, Marone E, Sepúlveda H (2018) Estimation of extreme wave heights return period from short-term interpolation of multi-mission satellite data: application to the South Atlantic. *Ocean Sci.* 14(4), 1-11., <https://doi.org/10.5194/os-2017-81>
- Samayam S, Laface V, Annamalaisamy SS, Arena F, Vallam S and Gavrilovich PV (2017). Assessment of reliability of extreme wave height prediction models, *Natural Hazards Earth System Science* 17, 409–421, <https://doi.org/10.5194/nhess-17-409-2017>.
- Shamji VR, Aboobacker VM and Vineesh TC (2020) Extreme value analysis of wave climate around Farasan Islands, southern Red Sea. *Ocean Engineering* 207, 107395. <https://doi.org/10.1016/j.oceaneng.2020.107395>. Simiu E and Heckert NA (1996) Extreme wind distribution tails: a “peaks over threshold” approach. *Journal of structural engineering* 122(5), 539-547. [https://doi.org/10.1061/\(ASCE\)0733-9445\(1996\)122:5\(539\)](https://doi.org/10.1061/(ASCE)0733-9445(1996)122:5(539))
- Teena NV, Kumar VS, Sudheesh K, Sajeew R (2012) Statistical analysis on extreme wave height. *Nat. Hazards* 64, 223–236. <https://doi.org/10.1007/s11069-012-0229-y>
- Vanem E (2015) Uncertainties in extreme value modelling of wave data in a climate change perspective. *Journal of Ocean Engineering and Marine Energy* 1, 339-359. <https://doi.org/10.1007/s40722-015-0025-3>
- Vinoth J and Young IR (2011) Global estimates of extreme wind speed and wave height. *Journal of Climate* 24(6), 1647-1665. <https://doi.org/10.1175/2010JCLI3680.1>
- Viselli AM, Forristall GZ, Pearce BR and Dagher HJ (2015) Estimation of extreme wave and wind design parameters for offshore wind turbines in the Gulf of Maine using a POT method. *Ocean Engineering* 104, 649-658. <https://doi.org/10.1016/j.oceaneng.2015.04>.
- WAFO (2000) A MATLAB toolbox for analysis of random waves and loads, Lund University, Sweden, homepage <http://www.maths.lth.se/matstat/wafo/2000>.

Table 1. Locations considered in the study, maximum significant wave height observed and the return level estimated using GEV-ML, GEV-PWM and GEV-PWM methods. Maximum value among the locations studied is indicated in bold letters.

Location	Position	Average SWH (m)	Maximum SWH (m)	RL - GEV ML (m)	RL - GEV PWM (m)	RL - GEV MPS (m)
L1	68.80°E,22.00°N	1.30	5.71	6.08	6.17	6.36
L2	69.80°E,21.00°N	1.31	7.87	7.00	7.18	7.77
L3	72.20°E,21.00°N	0.92	5.78	6.82	6.83	7.30
L4	72.20°E,20.00°N	1.17	6.59	6.77	7.07	7.30
L5	72.50°E,19.00°N	1.16	5.78	5.75	5.91	6.08
L6	72.50°E,18.00°N	1.29	5.78	6.05	6.03	6.35
L7	73.00°E,17.00°N	1.24	5.45	5.73	5.69	5.98
L8	73.20°E,16.00°N	1.22	5.25	5.70	5.69	5.94
L9	73.50°E,15.00°N	1.30	5.45	5.87	5.88	6.11
L10	74.00°E,14.00°N	1.29	5.44	6.04	6.03	6.26
L11	74.50°E,13.00°N	1.19	4.81	5.20	5.26	5.37
L12	75.00°E,12.00°N	1.00	4.26	4.25	4.34	4.45
L13	75.50°E,11.00°N	0.80	3.00	3.02	3.06	3.16
L14	76.00°E,10.00°N	1.10	4.53	4.43	4.48	4.73
L15	76.20°E,09.00°N	1.12	3.74	3.74	3.76	3.9
L16	77.50°E,08.00°N	1.49	3.75	3.71	3.65	3.83
L17	78.20°E,08.50°N	1.13	3.60	2.98	3.24	3.17
L18	80.00°E,11.00°N	0.79	4.09	4.4	4.39	4.72
L19	80.00°E,12.00°N	0.89	5.32	7.35	6.19	8.14
L20	80.30°E,13.00°N	0.94	5.36	8.46	6.73	8.74
L21	80.20°E,14.00°N	0.66	5.30	5.98	5.30	6.65
L22	80.20°E,15.00°N	0.74	5.55	6.82	5.99	7.36
L23	81.50°E,16.00°N	1.01	7.97	11.96	8.65	13.24
L24	82.50°E,17.00°N	0.89	4.09	5.00	4.84	5.27
L25	83.70°E,18.00°N	0.92	5.87	4.941	5.01	5.47
L26	85.00°E,19.00°N	1.17	7.28	8.06	7.74	8.88
L27	86.50°E,20.00°N	1.07	7.76	8.23	8.12	9.06
L28	87.00°E,21.00°N	0.75	5.55	7.42	6.76	7.81
L29	88.50°E,21.50°N	0.96	5.99	6.46	6.54	6.94
L30	90.00°E,21.50°N	1.19	7.90	10.04	10.01	10.75

Table 2. Locations considered in the study, maximum observed significant wave height, return level estimated using 91, 93, 95, 97 and 99 percentile and MRL plot following GPD. Maximum value is indicated in bold letters.

Locations	Maximum SWH (m)	RL -91 PERCENTILE (m)	RL -93 PERCENTILE (m)	RL -95 PERCENTILE (m)	RL -97 PERCENTILE (m)	RL -99 PERCENTILE (m)	RL-MRL (m)
L1	5.71	5.34	5.4	5.52	5.77	6.88	7.73
L2	7.87	6.17	6.16	6.25	6.61	8.02	8.24
L3	5.78	4.92	5.07	5.49	6.61	9.9	7.53
L4	6.59	5.57	5.63	5.84	6.51	8.26	8.75
L5	5.78	5.20	5.25	5.57	6.12	7.04	6.5
L6	5.78	5.47	5.56	5.83	6.54	7.11	6.69
L7	5.45	5.23	5.29	5.52	6.17	6.73	6.56
L8	5.25	5.17	5.23	5.41	5.76	6.88	6.99
L9	5.45	5.39	5.47	5.61	6.07	7.23	7.28
L10	5.44	5.42	5.51	5.71	5.99	7.14	7.24
L11	4.81	4.89	5.01	5.16	5.34	6.13	6.1
L12	4.26	4.08	4.12	4.24	4.38	4.74	5.44
L13	3.00	2.95	2.95	2.95	2.95	3.06	3.37
L14	4.53	4.15	4.22	4.31	4.48	5.07	5.26
L15	3.74	3.59	3.62	3.64	3.69	3.8	3.92
L16	3.75	3.61	3.61	3.63	3.68	3.84	3.99
L17	3.60	2.86	2.9	2.97	3.07	3.39	4.24
L18	4.09	5.69	5.97	6.7	7.31	5.77	5.41
L19	5.32	7.84	8.58	9.45	12.2	9.63	6.81
L20	5.36	13.02	14.73	17.03	19.19	18.18	7.48
L21	5.30	8.44	8.41	8.85	9.88	11.16	6.37
L22	5.55	17.33	18.63	20.41	17.24	9.77	6.43
L23	7.97	10.01	11.44	13.73	19.76	39.66	9.68
L24	4.09	7.67	8.17	8.64	9.56	7.58	5.68
L25	5.87	5.56	6.15	6.58	6.70	7.88	6.22
L26	7.28	9.17	10.16	10.99	10.77	11.91	8.92
L27	7.76	9.19	10.04	11.06	11.91	11.5	9.26
L28	5.55	14.74	17.61	19.19	15.11	10.63	7.62
L29	5.99	7.84	8.17	7.87	7.73	6.91	7.2
L30	7.90	8.43	8.41	8.91	9.75	9.83	8.3

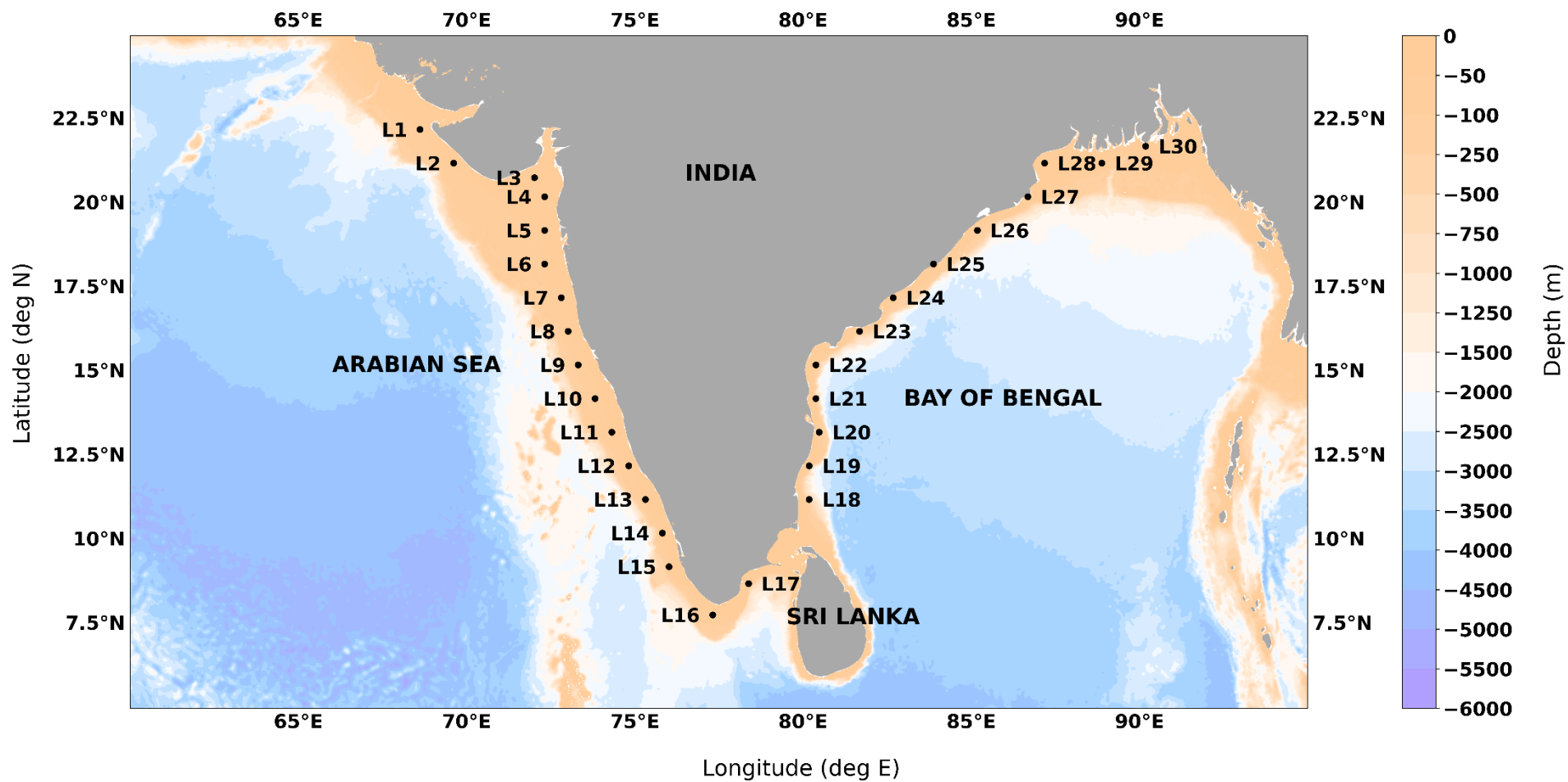


Figure 1. Map showing the study locations (L1 to L30) in the Indian shelf seas. The colour shade indicates the water depth in m.

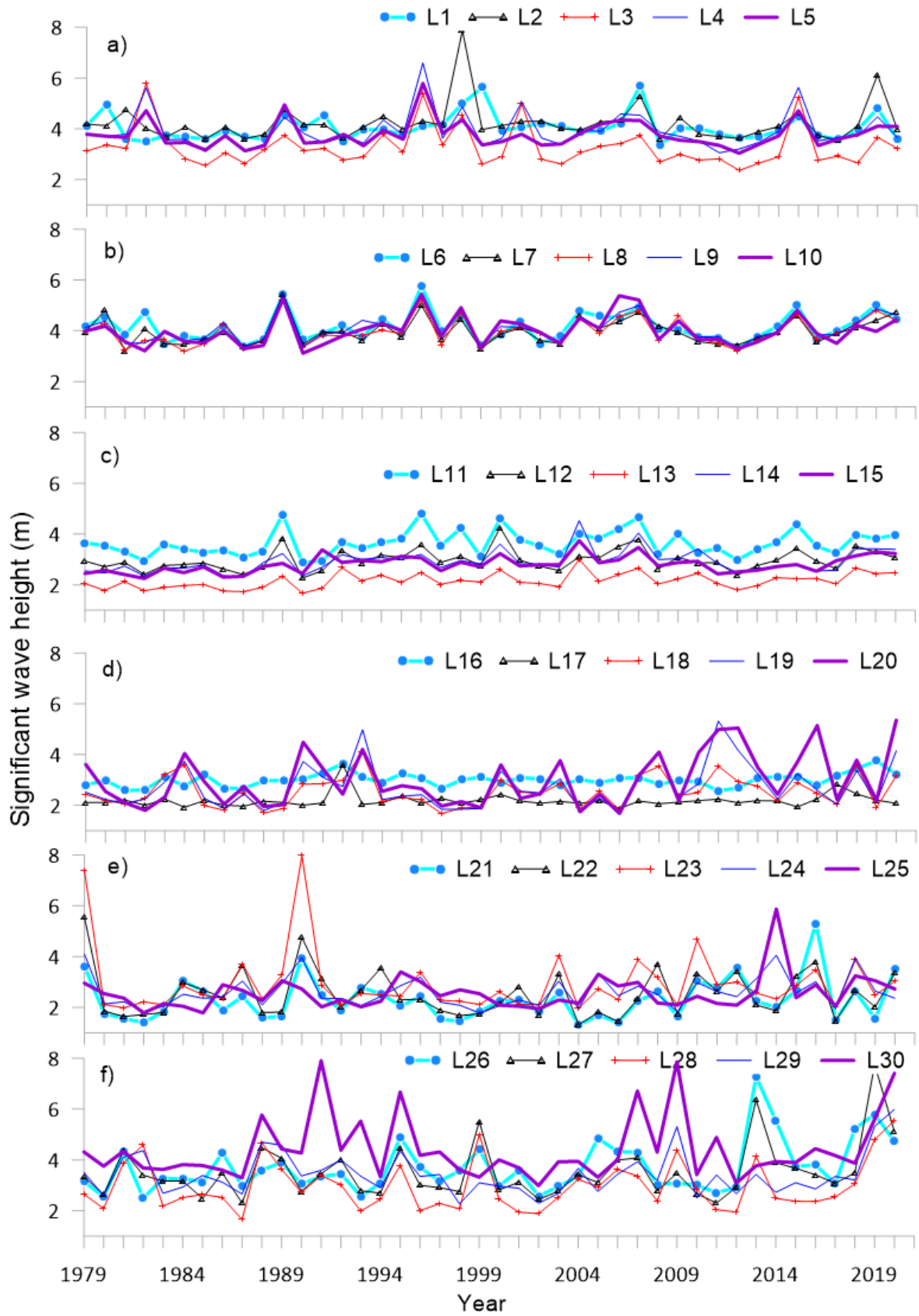


Figure 2. Annual maximum significant wave height in 30 locations around Indian Ocean from 1979 to 2021: (a) L1 – L5, (b) L6 – L10, (c) L11 – L15, (d) L16 – L20, (e) L21 – L25, (f) L26 – L30

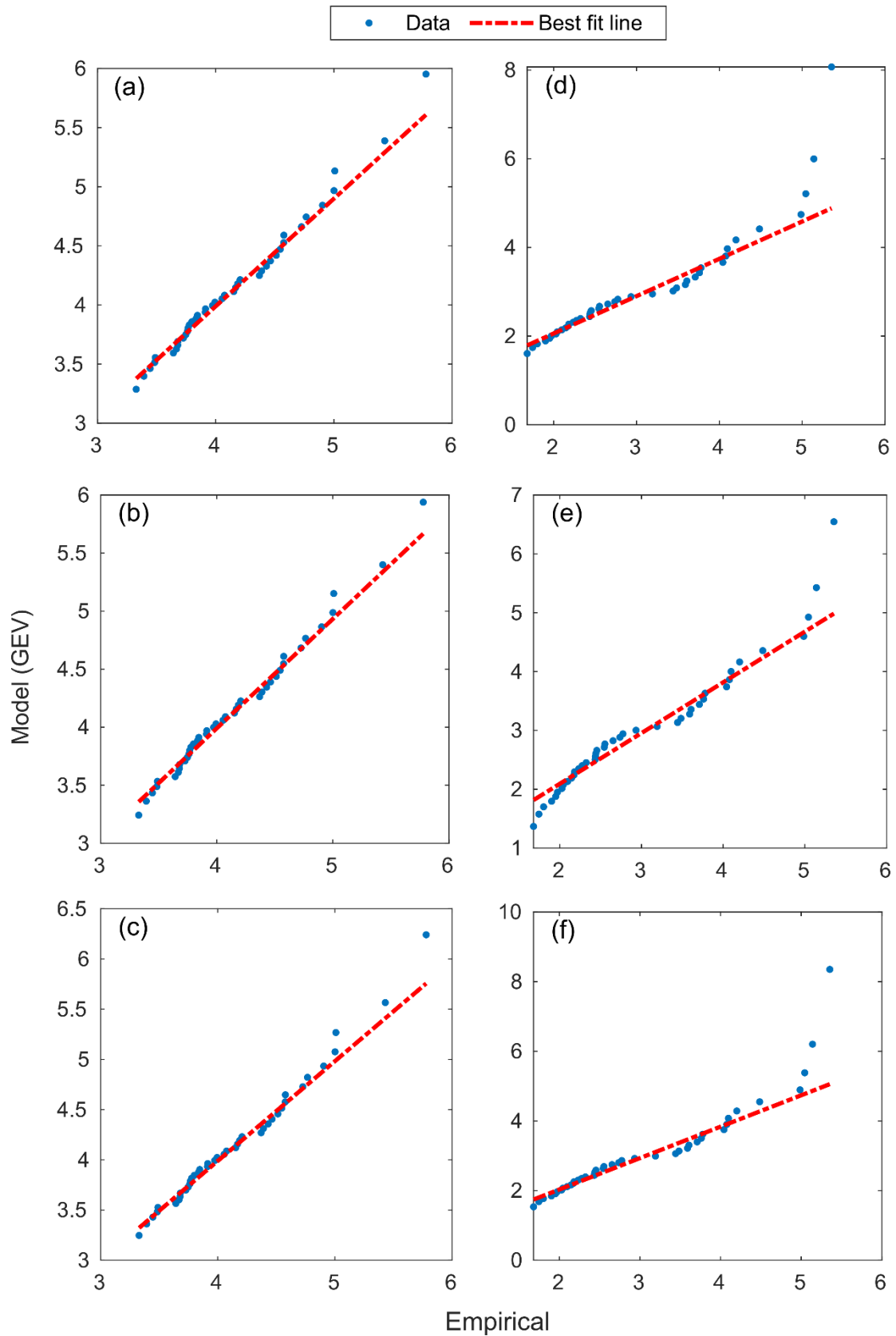


Figure 3. Residual quantile plot for typical locations by ML (a and d), PWM (b and e) and MPS method (c and f). Left panel is for location L6 and right panel is for location L20. Dots represents the wave height data.

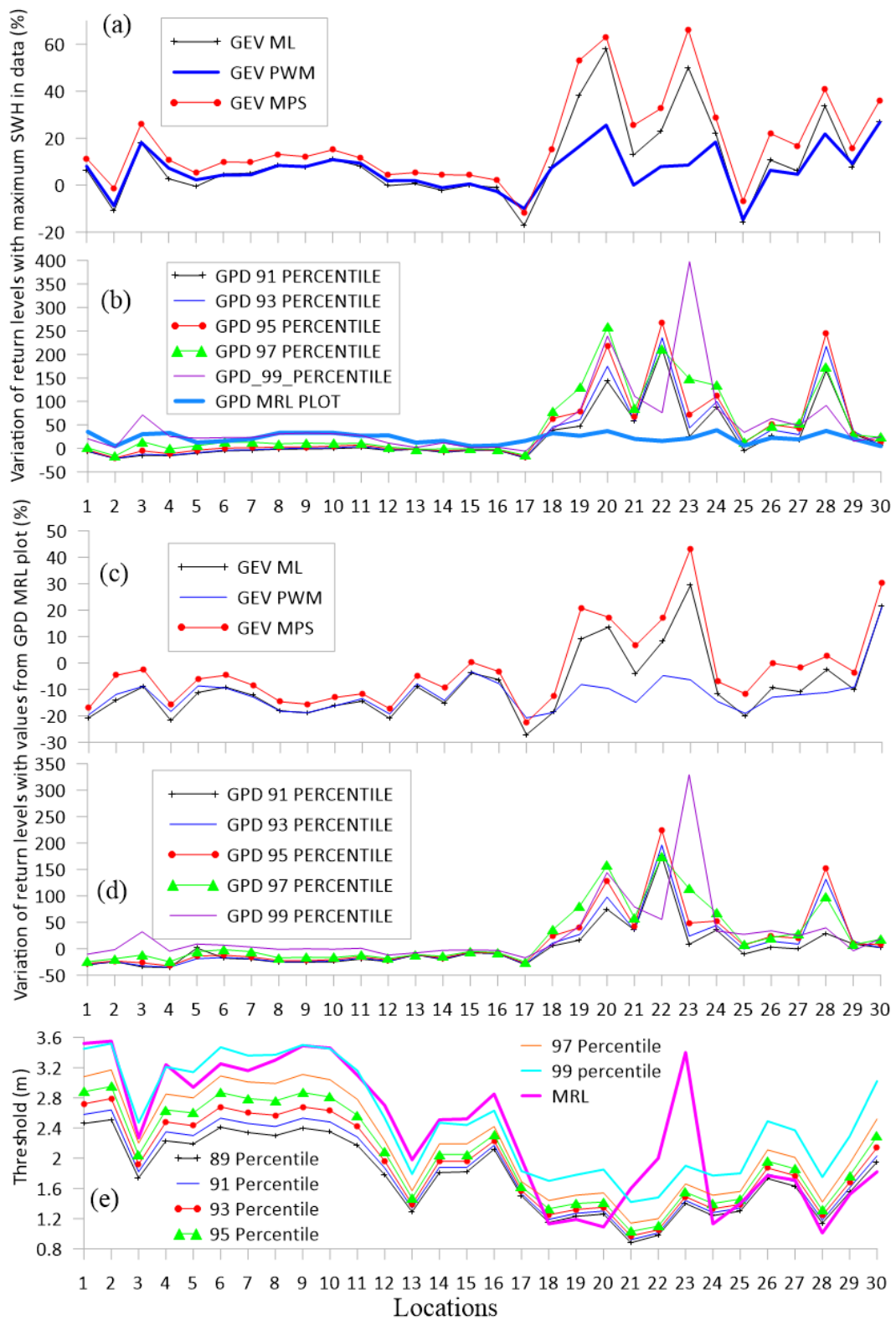


Figure 4. Percentage variation of return levels obtained from different methods using a) GEV and b) GPD compared to the maximum SWH in the data. c) values obtained from GEV ML, PWM and MPS compared to the value obtained from GPD MRL plot, d) values obtained from GPD with threshold 91, 93, 95, 97 and 99 percentiles with MRL plot, e) threshold values

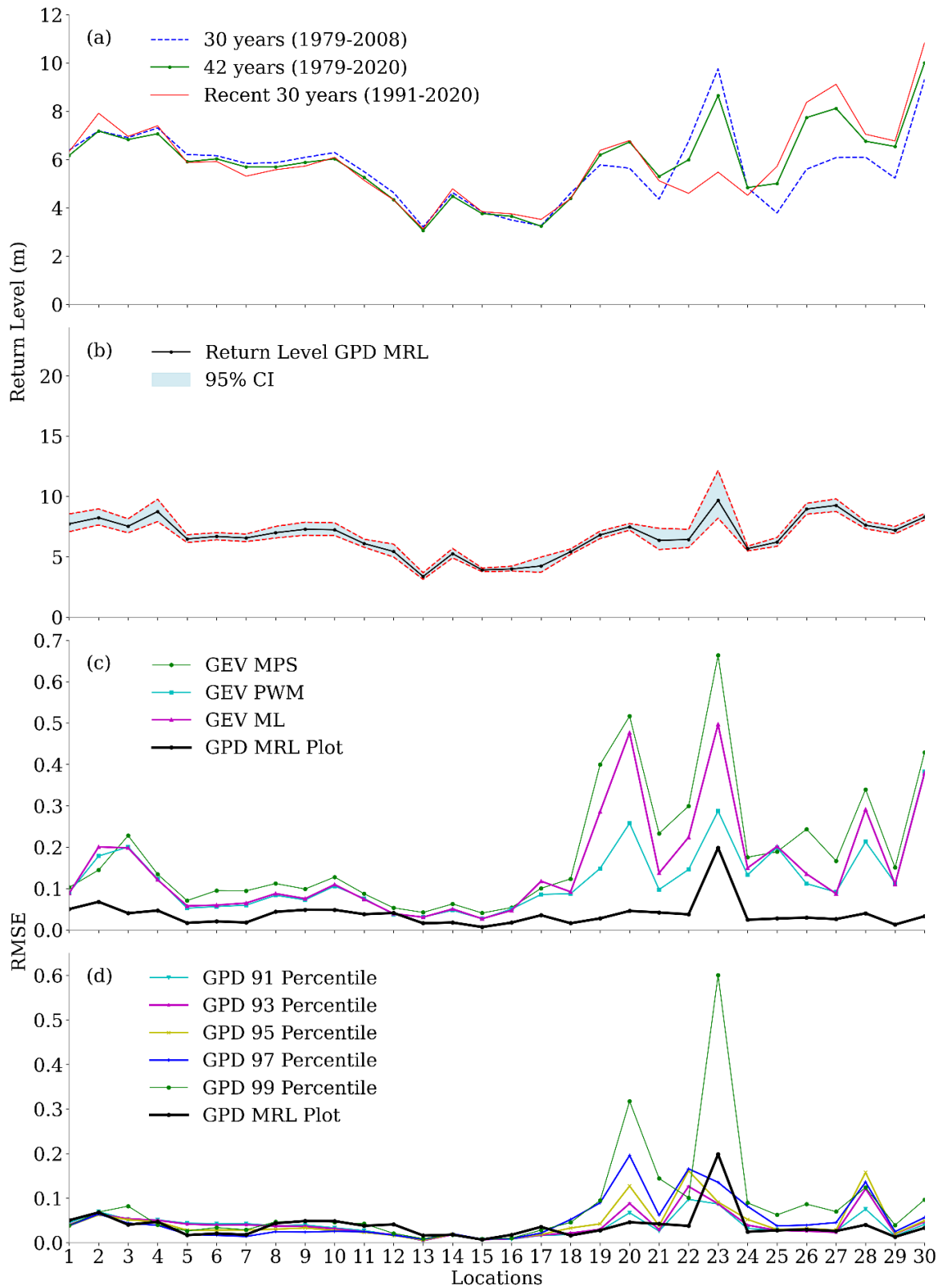


Figure 5. a) Return levels estimated using GEV PWM method with different datasets. b) Return levels estimated using GEV PWM with corresponding 95% confidence interval (CI). c) RMSE of return levels from different methods of GEV and GPD MRL method d) RMSE of Return levels with different methods of GPD.

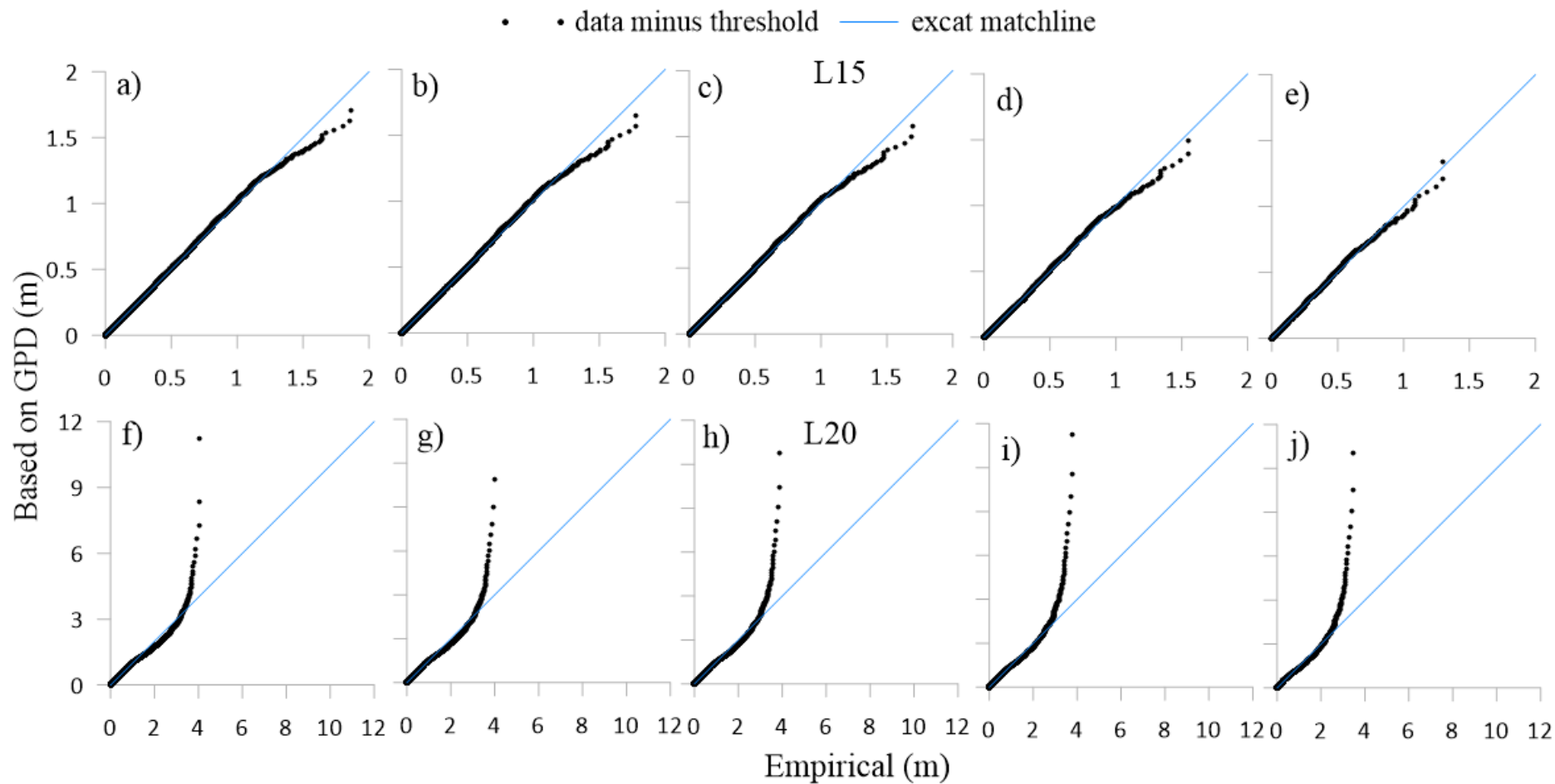


Figure 6. Residual quantile plots of a typical locations were threshold estimated using percentile method: a) and f) 91 percentile, b) and g) 93 percentile, c) and h) 95 percentile, d) and i) 97 percentile, e) and j) 99 percentile. Top panel is for location L15 and bottom panel is for location L20. Dots represents the wave height data minus the threshold value.

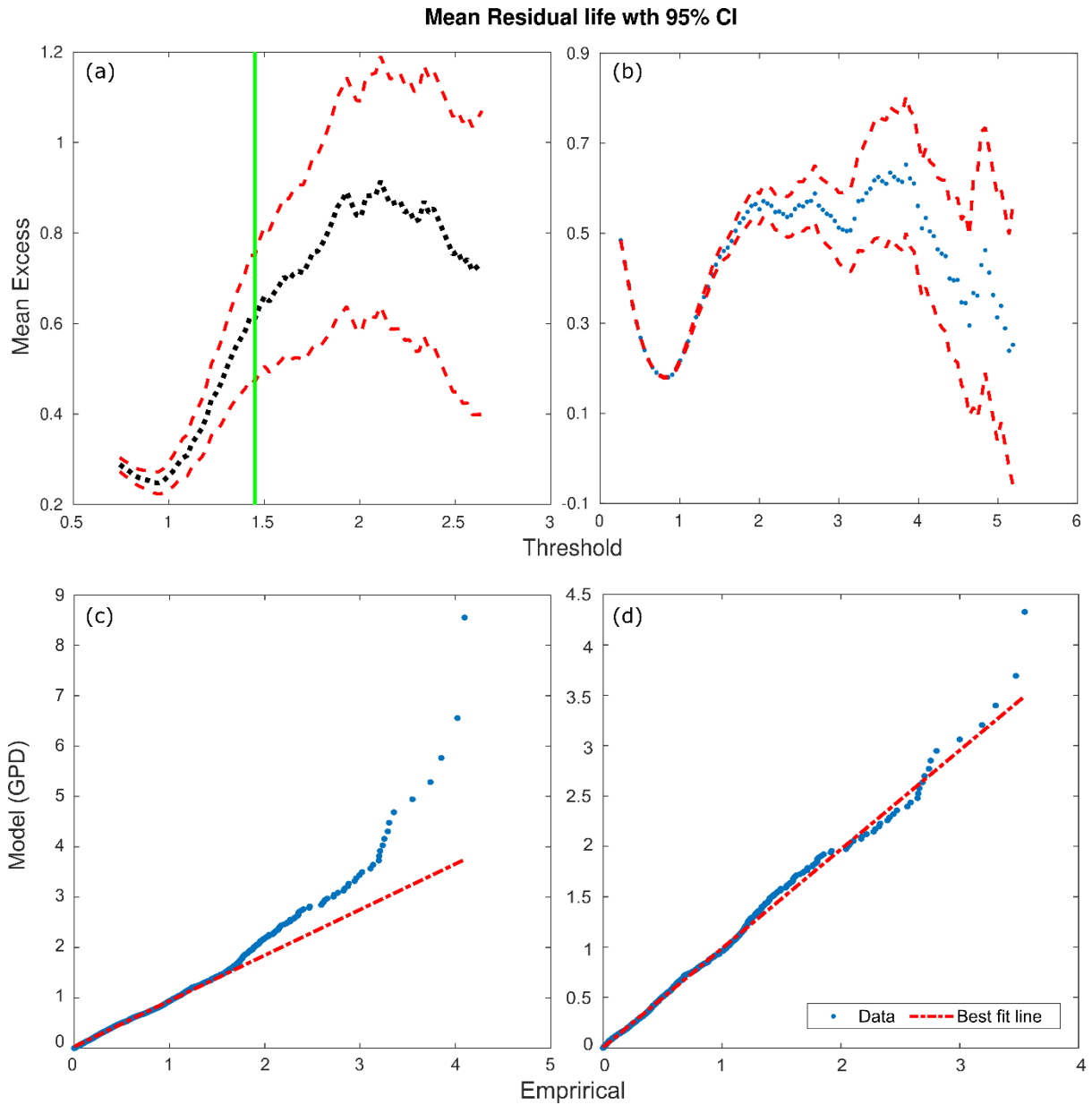


Figure 7. Top panel shows the threshold selection using mean residual life plot for location L22: (a) threshold estimation using mean residual analysis (green line represents the selected threshold) 1.45 m is the selected threshold, (b) threshold selection by manual visual inspection, the selected threshold is 2 m. Bottom panel shows the residual quantile plot for location L22 based on (c) threshold estimated using mean residual analysis, (d) threshold chosen manually